Local dielectric resonance and collective response of randomly ordered metallic cells in composites

2006 J. Phys.: Condens. Matter 18 4515

(http://iopscience.iop.org/0953-8984/18/19/007)

INSTITUTE OF PHYSICS PUBLISHING JOURNAL OF PHYSICS: CONDENSED MATTER

J. Phys.: Condens. Matter **18** (2006) 4515–4526 doi:10.1088/0953-8984/18/19/007

Local dielectric resonance and collective response of randomly ordered metallic cells in composites

L J Wang, Ying Gu, Bing Dai and Qihuang Gong

State Key Laboratory for Mesoscopic Physics, Department of Physics, Peking University, Beijing 100871, People's Republic of China

E-mail: ygu@pku.edu.cn and qhgong@pku.edu.cn

Received 25 December 2005, in final form 3 April 2006
Published 25 April 2006
Online at stacks.iop.org/JPhysCM/18/4515

Abstract

We investigate the dielectric resonance, local field distribution and optical response of randomly ordered nanometre metallic cells in two-dimensional composites using the Green's function formalism. It is found that the microstructure of a single cell determines the bandgap profiles of dielectric resonances, showing that these metallic cells have locally resonant structures. One or several defect bonds are introduced into each cell, expressed as the difference admittance ratio $\eta = (\epsilon_2 - \epsilon_0)/(\epsilon_1 - \epsilon_0)$. With varying η, the resonance bandgaps and effective optical absorption spectra are modified according to the single cell response, or local resonance structure. However, near resonances, the local field distributions from the localized modes to extended modes are shown to be the collective response of the whole material, rather than a single cell response. The results will be beneficial to the study of surface plasmon resonances in nanometre metallic clusters.

(Some figures in this article are in colour only in the electronic version)

1. Introduction

Photonic crystals have attracted great interest due to the existence of photonic band gaps [1–3]. In periodically arranged dielectric materials, light of allowed modes can transmit the materials, while others are almost completely inhibited. Recently, metallic–dielectric photonic crystals, where at least one component possesses the negative dielectric constant, have also attracted attention [4–8]. In some metallic–dielectric photonic crystals, the bandgap could begin almost at the zero frequency, and there is a cutoff frequency in the transmission spectrum [4, 5]. When defects are introduced into metallic–dielectric materials, some particular light modes will appear, having an obvious effect on the transmittance, absorption, refraction and reflection [6, 7].

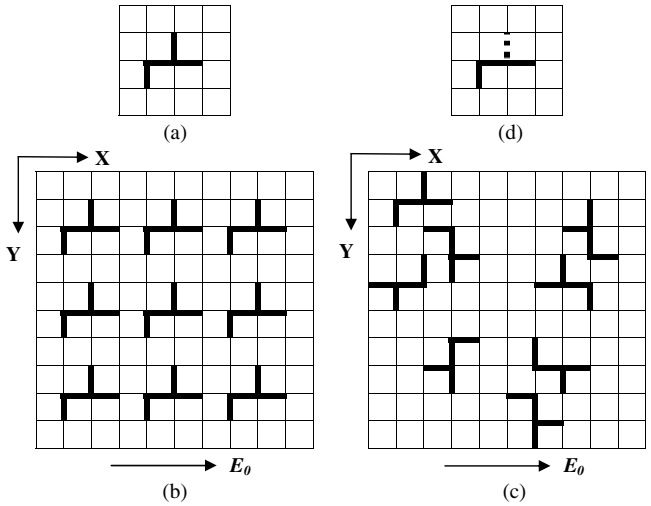

Figure 1. Schematic diagram of metallic cells (ϵ_1), shown in thick lines, embedded in a 2D dielectric network (ϵ_0): (a) single cell; (b) periodically arranged cells [19]; (c) randomly arranged cells; and (d) coloured cell (one bond is different from the others, with admittance ϵ_2).

In the quasistatic limit, due to the simultaneous existence of positive and negative admittance in metallic–dielectric composites, many dielectric resonances happen [9, 10]. Near resonance, the electric field is very localized within and around the impurity metallic clusters [11] and strongly enhances the effective linear and nonlinear optical responses [12–14]. These resonances exist both in isolated clusters [11] and in various disordered composites [15, 16], appearing as a very localized field distribution, or 'hot' spots [17, 18]. In periodic metallic arrays, the bandgaps of dielectric resonance and very localized defect modes have been reported [19]. Also, in the fractal structured metallic–dielectric composites, similarities of dielectric resonance, local field distribution and optical response have been predicted [20]. Then, for a structure between random and regular, what would the dielectric resonance properties be? To answer this question, in the present study we investigate the dielectric resonance spectra and optical responses of random metallic cells in metallic–dielectric composites.

In the discrete metallic–dielectric lattice model, it is well known that the number of metallic bonds equals the number of dielectric resonances, while its micro geometry determines the position of resonances [9, 11, 14]. For example, consider a single cell cluster with four bonds, as shown in figure 1(a). There are four dielectric resonances, as in figure 2(a). Our numerical calculations indicate that, in the periodic arrays (figure 1(b)), the bandgap profiles of dielectric resonances as in figure 2(b) [19] correspond to those found in a single cell, as well as in the randomly arranged metallic cells in figure 2(c). That is to say, the microstructure of a single cell approximately determines the resonance properties of the whole system, which is a phenomenon that we call local dielectric resonance. This kind of local resonance has been reported in sonic materials [21]. The local resonance mentioned here is different from the general localization of resonance in that, in general cases, the electric field is very localized in the metallic clusters when resonance occurs.

In the following, using the Green's function formalism (GFF) in the two-dimensional (2D) network composite [11, 15], we describe our investigations of the dielectric resonance, local field distribution near resonance, and optical response of random metallic cells with admittance

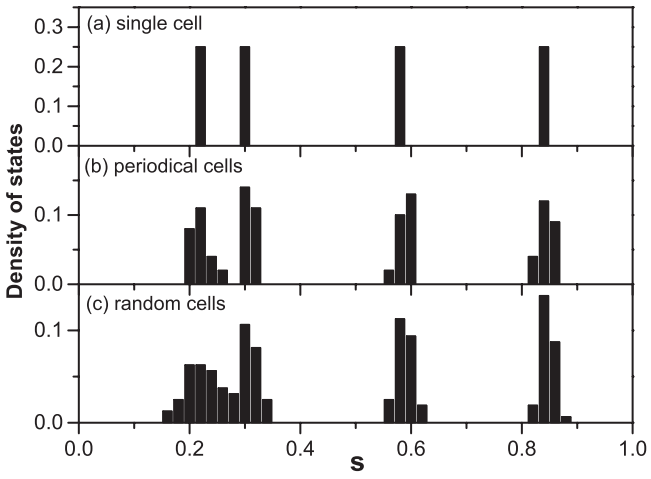

Figure 2. DOS (density of states) of dielectric resonances: (a) single cell; (b) periodically arranged cells; and (b) randomly arranged cells. s $(=\frac{1}{1-\epsilon_1/\epsilon_0})$ is the eigenvalue of matrix $\tilde{M}$.

ϵ_1 embedded in the dielectric host with ϵ_0. Several bandgaps appear in the dielectric resonance spectrum. The number of bandgaps is determined by the micro geometry of a single cell due to the local dielectric resonance of metallic cells. Then, one or several defect bonds with ϵ_2 are introduced into each cell, expressed as the difference admittance ratio [15] $\eta = \frac{\epsilon_2-\epsilon_0}{\epsilon_1-\epsilon_0}$. When η varies from $+\infty$ to $-\infty$, one or several branches of dielectric resonances change correspondingly from $+\infty$ to $-\infty$, leading to the modification of resonance bandgaps and of optical responses. Simultaneously, we check the local field distribution near resonances. Our numerical calculations indicate that, near resonances, the local field distributions from the localized mode to the extended mode are shown to be the collective response of the whole material, rather than a single cell response. These results will be beneficial to the study of surface plasmon resonances in nanometallic clusters.

The paper is organized as follows. In section 2, we first review the GFF of two- and three-component composites in 2D networks; then the local dielectric resonance for random metallic cells is proposed. In section 3, when the defect bonds are introduced into each cells, the resonance bandgap modification is presented. In section 4, we calculate the optical responses of random cells with varying η. In section 5, the inverse participation ratio (IPR) (which is used to represent the localization of the field) and the corresponding local field distributions near resonances are given. Finally, we summarize the main results in the last section.

2. Local dielectric resonance of random cells

2.1. Review of Green's function formalism

A Green's function method was developed to analyze the static macro conductance by solving Kirchhoff's equations in the resistor networks [22]. Here we use the Green's function formalism to compute the resonant properties of binary and three-component network composites in two dimensions (2D) and three dimensions (3D) [11, 14, 15]. The salient properties of GFF are first reviewed. As shown in figures 1(a) and (d), referring to [11, 15], the impurity metallic clusters of admittance ϵ_1 are employed to replace bonds of an otherwise homogeneous network of identical admittance ϵ_0. In this lattice model, the bonds are assumed

to be infinitely thin and the lattice constant is on the nanometre scale, which is much smaller than the wavelength of visible light. Here, solid thick lines are used to represent the metallic bonds with ϵ_1. In the Drude free electronic model, the admittance ϵ_1 is frequency dependent and always negative below the plasma frequency. For the rest of the metallic cells, the bonds have the admittance ϵ_0 and they are always assumed to be unity. For a unit point source placed at site $\mathbf{0} = (0, 0)$ outside a set of clusters of n_s sites, in the quasi-static limit, the electric potential V satisfies the Kirchhoff equation

$$\sum_{\vec{\mathbf{y}}(\vec{\mathbf{x}})} \epsilon_{\vec{\mathbf{x}},\vec{\mathbf{y}}}(V_{\vec{\mathbf{x}},\mathbf{0}} - V_{\vec{\mathbf{y}},\mathbf{0}}) = \delta_{\vec{\mathbf{x}},\mathbf{0}}, \tag{1}$$

where $\vec{\mathbf{x}} = (x_1, x_2)$ and $\vec{\mathbf{y}}(\vec{\mathbf{x}})$ denotes the four nearest neighbouring sites of $\vec{\mathbf{x}}$; $V_{\vec{\mathbf{x}},\mathbf{0}}$ is the electrostatic Green's function at $\vec{\mathbf{x}}$ due to the point source, and $\epsilon_{\vec{\mathbf{x}},\vec{\mathbf{y}}} = \epsilon_{\vec{\mathbf{y}},\vec{\mathbf{x}}}$ is the admittance of the bond joining the neighbouring sites $\vec{\mathbf{x}}$, $\vec{\mathbf{y}}$. Let $v = 1-\epsilon_1/\epsilon_0$; equation (1) can be transformed to a general form:

$$V_{\vec{\mathbf{x}},\mathbf{0}} = \frac{G_{\vec{\mathbf{x}},\mathbf{0}}}{\epsilon_0} + v\sum_{\vec{\mathbf{y}}\in C} M_{\vec{\mathbf{x}},\vec{\mathbf{y}}} V_{\vec{\mathbf{y}},\mathbf{0}}, \tag{2}$$

where $M_{\mathbf{x},\mathbf{y}} = \sum_{\mathbf{z}\in C(\mathbf{y})} (G_{\mathbf{x},\mathbf{y}} - G_{\mathbf{x},\mathbf{z}})$, and $G_{\vec{\mathbf{x}},\vec{\mathbf{y}}}$ is the Green's function of a Laplace operator on a square lattice, i.e., $-\Delta G_{\mathbf{x},\mathbf{y}} = \delta_{\mathbf{x},\mathbf{y}}$ with $G_{\mathbf{x},\mathbf{x}} = 0$. The microstructure of impurity metallic clusters is completely mapped by the square matrix $\tilde{M}$ in the clusters subspace. Then nontrivial eigenvalues s $(=\frac{1}{1-\epsilon_1/\epsilon_0})$ of $\tilde{M}$ construct the dielectric resonance spectrum. For a binary metallic–dielectric network, the resonance is restricted in the range $0 \leqslant s \leqslant 1$ and $\frac{\epsilon_1}{\epsilon_0}$ has a branch cut in the negative real axis [9, 11]. Then the third component ϵ_2 (or a defect cluster C_2) is introduced into the clusters, expressed by a difference admittance ratio $\eta = \frac{\epsilon_2-\epsilon_0}{\epsilon_1-\epsilon_0}$, shown as the dashed line in figure 1(d). The element of Green's matrix $\tilde{M}$ becomes [15] $\tilde{M}_{\mathbf{x},\mathbf{y}} = \sum_{\mathbf{z}\in C_1(\mathbf{y})}(G_{\mathbf{x},\mathbf{y}} - G_{\mathbf{x},\mathbf{z}}) + \eta\sum_{\mathbf{z}\in C_2(\mathbf{y})}(G_{\mathbf{x},\mathbf{y}} - G_{\mathbf{x},\mathbf{z}})$, where C_i means the ith cluster. The Green's matrix $\tilde{M}$ is greatly modified with varying η. The eigenvalues of $\tilde{M}$ (or the dielectric resonances) are extended to $-\infty \leqslant s \leqslant \infty$. When η is negative, there exists at least one negative eigenvalue [15]. These dielectric resonances obey the 2D sum rule [9, 11, 23]: $\sum_{i=1}^{n} s_i = \frac{n_2}{2}\eta + \frac{n_1}{2}$, where n_1 is the number of bonds with the admittance ϵ_1, and n_2 is the number with ϵ_2.

When dielectric resonance occurs, the field is localized within and around the impurity metallic clusters. To remove the infiniteness near the resonance, the residue of the electrical potential is given as [11]

$$\text{Residue}(V_{\mathbf{x},0}) = \frac{1}{\epsilon_0}\left(\sum_{\mathbf{y}\in C} \tilde{L}_{m,\mathbf{y}}\tilde{G}_{\mathbf{y},0}\right)\left(\sum_{\mathbf{z}\in C} M_{\mathbf{x},\mathbf{z}}\tilde{R}_{m,\mathbf{z}}\right), \tag{3}$$

where $\tilde{R}_m$ and $\tilde{L}_m$ are the mth normalized right and left eigenvectors of the Green's matrix $\tilde{M}$. For more details, one can refer to [11, 15].

The GFF method was established in the quasi-static Kirchhoff equations, as well as other Green method [22] and the lattice models in [10, 24]. From the above description, the developed GFF in composite networks can not only give the dielectric resonances of the arbitrary metallic clusters, but can also give their local field distributions near resonances. While using the method of Kirchhoff Hamiltonians [24], $\epsilon_1 = -\epsilon_0$ is always assumed, and the scaling and fluctuations of the electric field moments in the percolating composites are reported.

To model the optical responses, the Drude free electronic model is commonly used to represent the frequency-dependent admittance with $\epsilon_1 = 1 - \frac{\omega_p^2}{\omega(\omega+i\gamma)}$, where ω_p is the plasma frequency, and γ is a damping constant. For metal, $\omega_p \approx 10^{16}$, which is in the ultraviolet. We

choose $\gamma = 0.05\omega_p$, which is the typical value for metal. Let $\epsilon_0 = 1.77$, which is the dielectric constant of water for model calculations. The range of optical responses is $\omega/\omega_p \in (0, 1)$. The defect admittance ϵ_2 changes with η accordingly. Subject to a uniform field E_0 (=1) along the x direction, in the quasi-static limit the effective linear optical responses (or the absorption) along the applied field can be expressed as the imaginary part of the effective coefficient ϵ_e [9, 12]:

$$\operatorname{Im}\epsilon_e = -\operatorname{Im}\sum_{n=1}^{n_s}\frac{\sum_{\mathbf{y}\in\mathbf{C}} L_{n,\mathbf{y}} y_1 \sum_{\mathbf{x},\mathbf{y}\in\mathbf{C}}(x_1 - y_1)(\tilde{R}_{n,\mathbf{x}} - \tilde{R}_{n,\mathbf{y}})}{\epsilon_0(s - s_n)}. \tag{4}$$

Let $\gamma_n = \sum_{\mathbf{y}\in\mathbf{C}} L_{n,\mathbf{y}} y_1 \sum_{\mathbf{x},\mathbf{y}\in\mathbf{C}}(x_1 - y_1)(\tilde{R}_{n,\mathbf{x}} - \tilde{R}_{n,\mathbf{y}})$, and it obeys the sum rule [9, 12]: $\sum_n \gamma_n = N_h$, where N_h is the number of horizontal bonds along the applied field.

2.2. Dielectric resonance bandgap of random cells

The resonant properties of regular structures have been studied. In periodic arrays, there exist bandgaps of dielectric resonances [19], while in fractals the similarity of dielectric resonance distribution is predicted [20]. Now we want to know the dielectric resonance of randomly ordered metallic cells, whose structure is between regular and random. Numerical calculations indicate that the resonant properties of random cells are more like those found in the periodic arrays. The main reason is that the bandgap profiles of random cells are determined by the dielectric resonance of a single cell, exhibited as the local dielectric resonance mentioned above. Here, the four-bond metallic cell is only a representation of the arbitrary shaped clusters, rather than an oddly shaped metallic cluster or a particularly shaped cluster.

Figure 2 displays the density of states (DOS) of dielectric resonances of a single cell, periodic arrays, and random cells in 2D metallic–dielectric networks. Here, the statistical interval of resonances is $\Delta s = 0.02$ and the region $s \in (0, 1)$. In the periodic arrays, the sample size is 30×30 and the concentration of the metallic part is $p = 20\%$. The metallic cells are randomly distributed in the dielectric host with the same size and concentration as the periodic arrays and without any sticking between them. In figures 2(b) [19] and (c), the dielectric resonance bandgaps appear in the spectrum of s. As shown in figure 2(a) the DOS of each state is 0.25, and in figures 2(b) and (c) the sum of each resonance band is also normalized to 0.25. The resonance branches correspond to the dielectric resonances of a single cell. Both in the periodic arrays and in random cells, the bandgap profiles of dielectric resonance are determined by the microstrucure of a single cell, shown as a local dielectric resonance. This is similar to the local resonance of sonic materials reported in [21]. The forming of the dielectric resonance bands can be regarded as the eigenvalues perturbation of a single cell by others. In a single metallic cell, the first and second resonances are very close. Then, in figure 2(c), due to the large perturbation, the first and second bands join together and the gap disappears. We also found that, with increasing concentration p of metallic cells, the resonance bands become wider due to the larger perturbation of neighbouring cells.

3. Dielectric resonance bandgap modification with defects

In this section, we introduce one or several defect bonds into metallic cells. The resulting cells are called coloured cells. All coloured metallic cells have the same micro geometry, or the defect bonds with admittance ϵ_2 exist at the same position of each cell, as shown in figure 1(d). Then, what happens to their resonant properties? Generally, we use the difference admittance ratio η $(=\frac{\varepsilon_2-\varepsilon_0}{\varepsilon_1-\varepsilon_0})$ to represent the defect, instead of the admittance ϵ_2 [15]. We expect that the coloured metallic cells should also exhibit the local resonance properties. In this and in the next

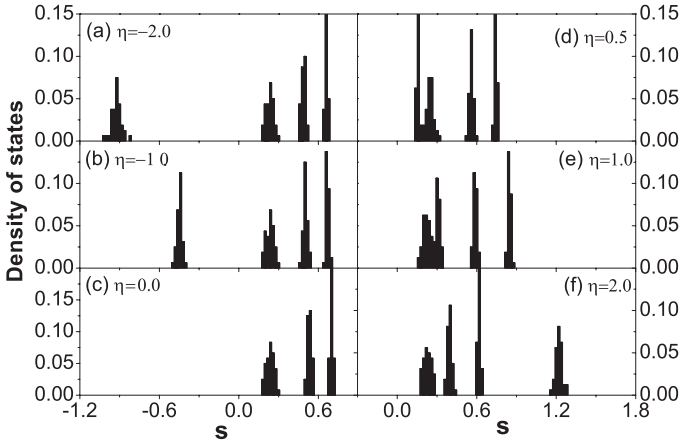

Figure 3. DOS of dielectric resonances for random metallic coloured cells with varying η ($=\frac{\epsilon_2-\epsilon_0}{\epsilon_1-\epsilon_0}$). Here, each coloured cell includes one defect bond. s ($=\frac{1}{1-\epsilon_1/\epsilon_0}$) is the eigenvalue of $\tilde{M}$.

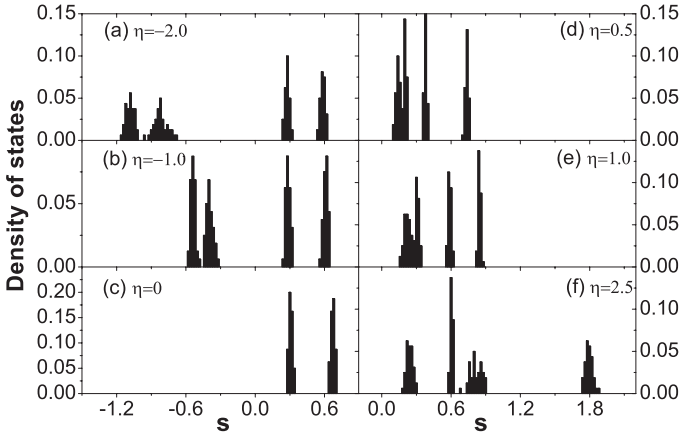

Figure 4. DOS of dielectric resonances for random metallic coloured cells with varying η ($=\frac{\epsilon_2-\epsilon_0}{\epsilon_1-\epsilon_0}$). Here, each coloured cell includes two defect bonds. s ($=\frac{1}{1-\epsilon_1/\epsilon_0}$) is the eigenvalue of $\tilde{M}$.

two sections, we investigate the effect of defect modes on the DOS, local field distribution near resonance, and the optical response of random metallic cells embedded in the dielectric host.

Figure 3 displays the DOS of dielectric resonances of random coloured cells with one defect bond. Here, $\eta = -2.0, -1.0, 0.0, 0.5, 1.0, 2.0$. When $\eta = -2.0$, one of four resonance bands is left-shifted due to the existence of the defect, as shown in figure 3(a), while for $\eta = 2.0$, one band is right-shifted, as shown in figure 3(d). Comparing $\eta = -2.0$ in figure 3(a) with $\eta = -1.0$ in figure 3(b), we find that, when η is smaller (or larger), one of the bands is more left-shifted (or right-shifted). When $\eta = 1.0$, the system once again becomes the binary, so the DOS spectrum in figure 3(e) is the same as that shown in figure 2(c). Another binary case is $\eta = 0.0$ in figure 3(c), where three dielectric resonance bands appear. When $\eta \in (0.0, 1.0)$, for example $\eta = 0.5$ in figure 3(d), the defect modes fall into the region $s \in (0.0, 1.0)$, leading to complicated modification of the bands. Then, in figure 4, we plot the DOS of random coloured cell with two defect bonds. Similar results are obtained. When η is larger or smaller, there

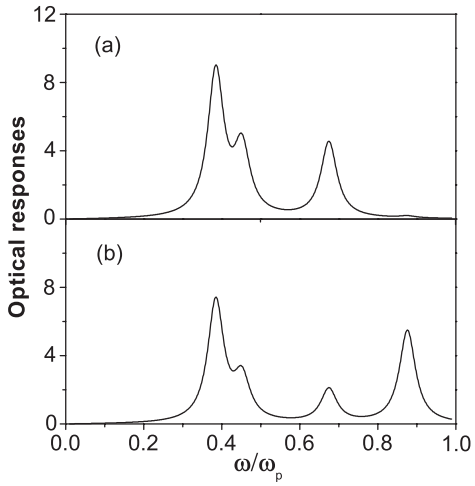

Figure 5. Effective linear optical responses for the single cell shown in figure 1(a), with 0° or 180° rotation shown in (a), and with 90° or 270° rotation shown in (b).

are two resonance bands left-shifted or right-shifted, as shown in figure 4(a) for $\eta = -2.0$ or figure 4(f) for $\eta = 2.5$. Comparing figure 4(a) for $\eta = -2.0$ with figure 4(b) for $\eta = -1.0$, we find that two bands are more left-shifted and have larger bandgaps. We can also conclude that, for the larger (or smaller) η, two bands are more left-shifted (right-shifted) and have larger bandgaps. When $\eta = 1.0$ in figure 4(e), the sample reverts to a binary case, the same as that in figures 3(e) and 2(c). But, for $\eta = 0.0$, it is also a binary case with two resonance bands. As was found in figure 3(d), for $\eta = 0.5$ as in figure 4(d), we almost could not distinguish the first and second bands and the bandgap, which indicates complicated behaviour.

From figures 3 and 4, we conclude that the resonance band modification of random coloured metallic cells is determined by the DOS spectra of a single coloured cell, also exhibiting a local dielectric resonance. When one or two resonance bands are shifted, other bands are kept almost at the original positions. Further numerical calculations indicate that, for the different configuration of defects in coloured cells, the modification of resonance bands with varying η has little difference. When η is large, the influence of defect parts is outside the region of optical responses, as shown in the following figures 6(e) and (f).

4. Optical response

Figure 5 displays the optical responses of a single cell. Since, in a single cell, there are four dielectric resonances, here the maximum four optical responses are shown. For a single cell in figure 1(a), there are two different configurations along the external field, so two kinds of responses are shown in figures 5(a) and (b), respectively. In the discussed metal–dielectric composites, the metallic cell is randomly distributed so, for each cell, a random configuration is chosen. The optical response of the whole system should be a superposition of two kinds of response. Considering a more general case, in figure 6 we give the statistical averaging of optical responses of the whole system.

Next, we introduce one defect bond in each cell. With varying η, in figure 6 we plot the effective linear optical responses of random metallic coloured cells. Here the sample size is 30×30. For each η, 5000 samples are used for the statistical averaging. We focus our attention

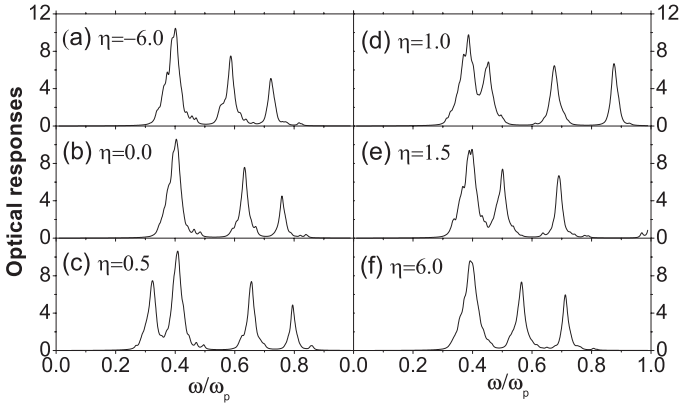

Figure 6. The statistical averaging of effective linear optical responses of random metallic cells with varying η ($=\frac{\epsilon_2-\epsilon_0}{\epsilon_1-\epsilon_0}$).

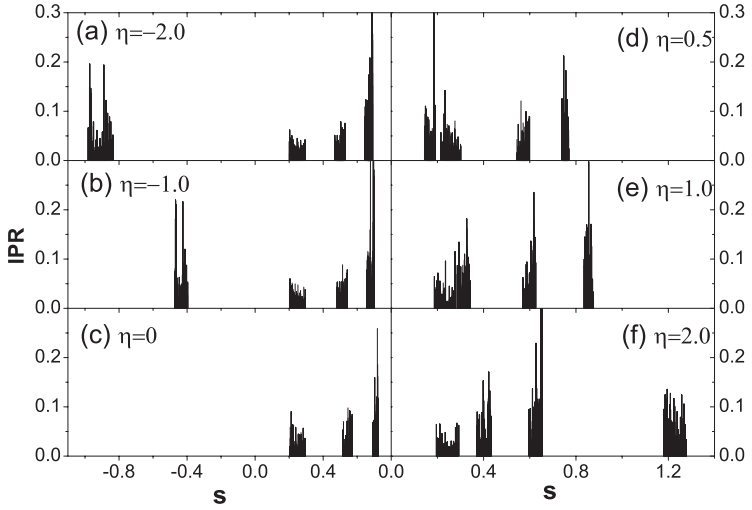

Figure 7. IPR of random metallic coloured cells with one defect bond at different η ($=\frac{\epsilon_2-\epsilon_0}{\epsilon_1-\epsilon_0}$).

on avoiding the crossing area [15] $\eta \in (0, 2)$. The modification of optical responses also shows the local resonance of a single coloured cell. When η is too small or too large, the influence of defects is out of the spectral region $\omega \in (0, 1)$, as shown in figures 6(a) and (f). At $\eta = 0.0$, the defects merge into the dielectric host and only three absorption peaks are left in figure 6(b), while at $\eta = 1.0$, four absorption peaks appear as shown in figure 6(d). For $\eta \in [0, 1]$, the defect modes are obviously within the area $\omega \in (0, 1)$, forming a four-peaked absorption spectrum, as shown in figure 6(c). For $\eta \in [1, 2]$, the defect modes fall approximately outside the region $\omega \in (0, 1)$, which influenced the positions of absorption peaks, instead of their intensities. So, when $\eta \in (0, 1)$, both the metallic bonds ϵ_1 and ϵ_2 contribute to the optical responses, while for $\eta \notin (0, 1)$, only the metallic bonds ϵ_1 work. This leads to about the same absorption profiles for both $\eta \to -\infty$ shown in figure 6(a) and $\eta \to +\infty$ in figure 6(f). However, as emphasized in figure 9, the main optical absorption peaks corresponds to the very extended local field, indicating a collective response.

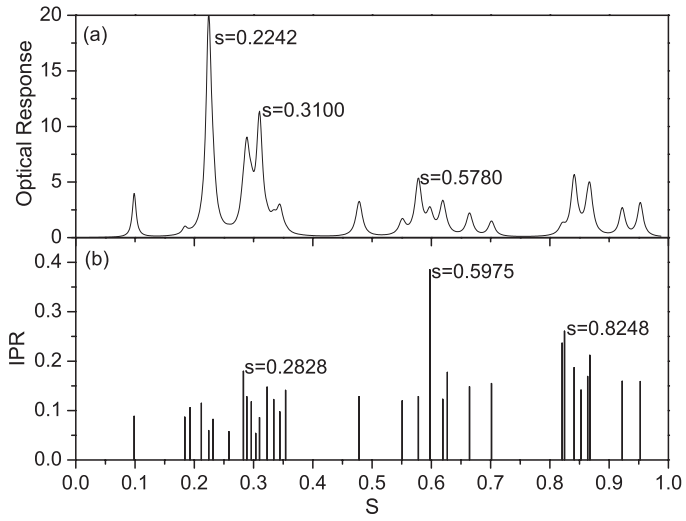

Figure 8. The optical response (a) and IPR (b) of random cells, as shown in the sample of figure 1(c). The eigenmodes with strong optical responses and with high values of IPR are flagged in the figure. s $(=\frac{1}{1-\epsilon_1/\epsilon_0})$ is the eigenvalue of $\tilde{M}$.

5. Local field distribution near resonance

From the above investigations, we know that the distribution of dielectric resonances and the static optical responses are determined by the single cell response; i.e., these metallic cells have a local resonant microstructure. If only a single cluster exists, when resonance happens, the electric field is localized within or around the metallic clusters [11]. However, for a composite containing many metallic cells, the field distributions near resonances do not clearly depend on one or several cells, indicating a collective response of the whole material. In this section, in order to expand our knowledge of the local field distribution near resonance, we first give the evolution of the inverse participation ratio (IPR) with varying difference admittance ratio η. Then, for a special sample figure 1(c), we give several 3D plots for the local field distributions of high optical response modes and high IPR modes to confirm that these eigenmodes (local fields) have the collective response of the whole material.

To represent the field localization, the IPR [25] with $q = 2$ of the right eigenvector is defined by $\mathrm{IPR}(R_n) = \sum_{i=1}^{n_s} {R_{n,i}}^4$, where $\langle {R_n}^2 \rangle = 1$. The higher value of IPR represents a more localized field, while the lower value of IPR represents the very extended field distribution. Figure 7 displays the IPR of random metallic coloured cells with one defect bond at different η, using a 30×30 sample. From the figure, we can see that most of the eigenmodes have very low IPR values, below 0.1. Only a very few of them have high IPR values. With varying η from -2.0 in figure 7(a) to 2.0 in figure 7(f), though the defect resonance band is moving, the distribution of IPR values do not have much adjustability. Please note that the IPR could not reflect the intensity of the electric field, so the high value of IPR could not represent the strong optical responses, because in the IPR calculations the intensity of the local field is normalized. The following example demonstrates this point directly.

Figure 1(c) is a typical sample of random metallic cells. Though its size is small (only 10×10), it is enough to represent the optical response and local field distribution of random metallic cells, but it is convenient to compare the positions of cells with the local field distribution. As shown in figure 8, the optical responses and the IPR distribution have features

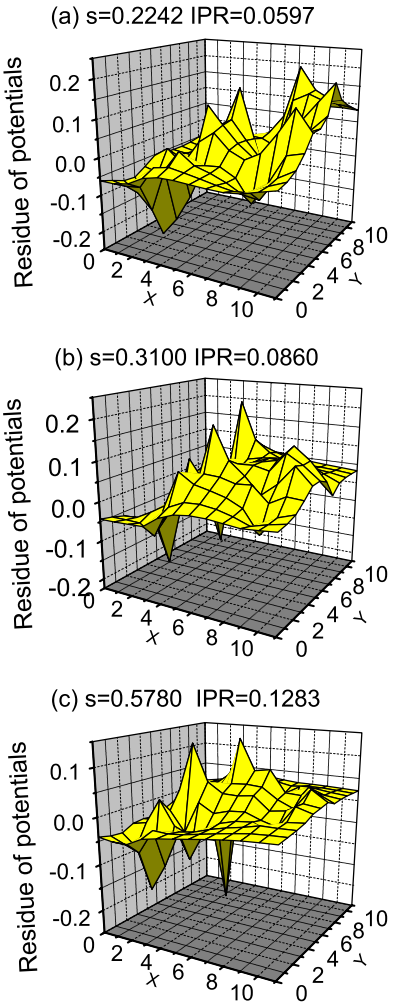

Figure 9. 3D plots of local field distributions with strong optical response states: (a) $s = 0.2242$ and IPR $= 0.0597$; (b) $s = 0.3100$ and IPR $= 0.0860$; and (c) $s = 0.5780$ and IPR $= 0.1283$.

similar to the larger samples (expressed as a statistical averaging). The electric potentials of the sites can be computed directly using equation (3). Figure 9 shows the 3D plots of local field distributions corresponding to three main absorption peaks in figure 8(a). In figure 9(a), $s = 0.2242$ and IPR $= 0.0597$; in figure 9(b), $s = 0.3100$ and IPR $= 0.0860$; and in figure 9(c), $s = 0.5780$ and IPR $= 0.1283$. It is seen that, for large optical responses, the fields have very extended distributions, which are expressed as the lower IPR values in figure 8(b). Comparing them with figure 1(c), we conclude that there is no obvious correspondence between the metallic cells and the field distribution. Then, in figure 10, we give the 3D plots of local field distributions with high IPR values. As shown in figure 8(b), $s = 0.5975$ and IPR $= 0.3851$ in figure 10(a); $s = 0.8248$ and IPR $= 0.2608$ in figure 10(b); and $s = 0.2828$ and IPR $= 0.1798$ in figure 10(c). The figures indicate that the fields are localized within very small areas, but their intensities are much smaller than those extended fields contributing to the absorption peaks. In these modes, we could not obtain the obvious correspondence between the metallic cells and

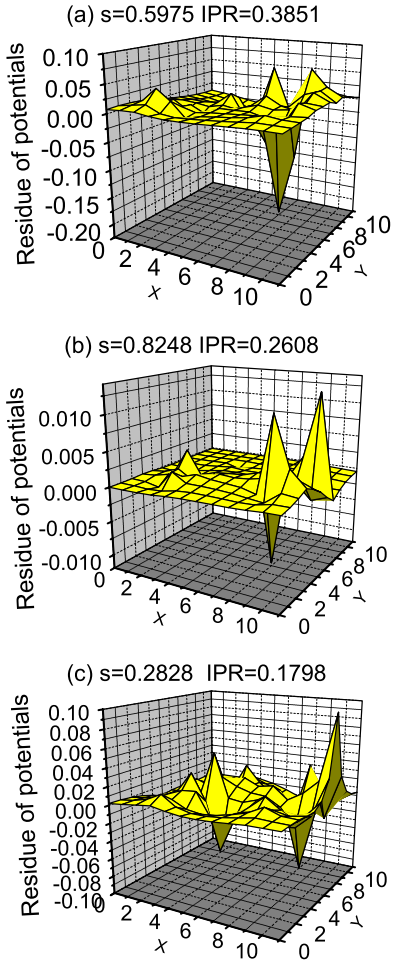

Figure 10. 3D plots of local field distributions with high IPR value states: (a) $s = 0.5975$ and IPR $= 0.3851$; (b) $s = 0.8248$ and IPR $= 0.2608$; and (c) $s = 0.2828$ and IPR $= 0.1798$.

localized fields. Therefore, we conclude that the local field distributions near resonances show a collective response of the whole material.

6. Summary

In this work, we have investigated the dielectric resonance, optical response, and local field distribution of randomly ordered metallic cells in composite materials. On the one hand, it is found that the microstructure of single cells determines the bandgap profiles of dielectric resonances and the optical responses, showing that these metallic cells have a locally resonant structure. When we introduce one or several defect bonds into each cell (expressed as the difference admittance ratio $\eta = (\epsilon_2 - \epsilon_0)/(\epsilon_1 - \epsilon_0)$), the resonance bandgaps and effective optical absorption spectra are still modified according to the single cell response. On the other hand, near resonances, the local field distributions from the localized modes to the extended modes are shown to be the collective response of the whole material, rather than a single

cell response. These results will be beneficial to the study of surface plasmon resonances of nanometre metallic clusters.

Acknowledgments

This work was supported by the National Natural Science Foundation of China under grant Nos 10334010, 10304001, 10521002, 10434020, 10328407 and 90101027.

References

[1] Yablonovitch E 1987 *Phys. Rev. Lett.* **58** 2059
[2] John S 1987 *Phys. Rev. Lett.* **58** 2486
[3] Sakoda K 2001 *Optical Properties of Photonic Crystals* (Berlin: Springer)
[4] Sigalas M M, Chan C T, Ho K M and Soukoulis C M 1995 *Phys. Rev.* B **52** 11744
[5] Sievenpiper D F, Yablonovitch E, Winn J N, Fan S, Villeneuve P R and Joannopoulos J D 1998 *Phys. Rev. Lett.* **80** 2829
[6] Sievenpiper D F, Sickmiller M E and Yablonovitch E 1996 *Phys. Rev. Lett.* **76** 2480
[7] Gadot F, Lustrac A and Lourtioz J 1999 *J. Appl. Phys.* **85** 8499
[8] Shen J T and Platzman P M 2004 *Phys. Rev.* B **70** 035101
[9] Clerc J P, Giraud G, Luck J M and Robin T 1996 *J. Phys. A: Math. Gen.* **29** 4781
[10] For a review, see Bergman D J and Stroud D 1992 *Solid State Physics* vol 146, ed H Ehrenreich and D Turnbull (New York: Academic) p 147
[11] Gu Y, Yu K W and Sun H 1999 *Phys. Rev.* B **59** 12847
[12] Gu Y and Yu K 2002 *Chin. Phys.* **11** 0601–7
[13] Gu Y and Gong Q H 2002 *J. Phys.: Condens. Matter* **14** 6567
[14] Dai B, Gu Y, Li C and Gong Q H 2004 *Eur. Phys. J.* B **42** 165
[15] Gu Y and Gong Q 2003 *Phys. Rev.* B **67** 014209
[16] Gu Y, Yu K W and Yang Z R 2002 *Phys. Rev.* B **66** 012202
[17] Stockman M I 1997 *Phys. Rev.* E **56** 6494
[18] Sarychev A K, Shubin V A and Shalaev V M 1999 *Phys. Rev.* B **60** 16389
[19] Gu Y and Gong Q 2004 *Phys. Rev.* B **70** 092101
[20] Dai B, Gu Y, Li C and Gong Q 2005 *Phys. Rev.* B **72** 064112
[21] Liu Z, Zhang X, Mao Y, Zhu Y Y, Yang Z, Chan C T and Sheng P 2000 *Science* **289** 1734
[22] Bergman D J and Kantor Y 1981 *J. Phys.: Condens. Matter* **14** 3365
[23] Gu Y and Gong Q 2004 *Phys. Rev.* B **69** 035105
[24] Sarychev A K and Shalaev V M 2000 *Phys. Rep.* **335** 275
[25] Wegner F 1980 *Z. Phys.* B **36** 209